

Jahanger HK

*Cardiff University
School of Engineering*

Robson S

*Cardiff University
School of Engineering*

Haddad M

*Cardiff University
School of Engineering*

Sumner M

University of Nottingham

SUSTAINABLE ENERGY

Double-ended Fault Location Method with Reduced Measurements

The double-ended impedance-based fault location Method (DEFLM) uses the wideband frequency content of the transient generated by the fault to determine the impedance from the point of measurement to the fault. This work evaluates the use of DEFLM in integrated power system such as those in More Electric Vehicles. Two approaches have been investigated with two measurements from two terminals and with one reduced measurement. The outcomes demonstrate that the DEFLM with full measurements provide a very high accuracy of the fault location with accuracy reaches 99% assuming the two end measurements are synchronized. On the other hand, the DEFLM with reduced current measurement from loads end shows less accuracy as the fault reaches the load terminal. However, the accuracy still high and within acceptable range utilizing more cost-effective approach.

Keywords:

Double-ended, fault location, high frequency, impedance-estimation, transient.

Corresponding author:

JahangerJ@cardiff.ac.uk



H.K. Jahanger, S. Robson, M. Haddad, and M. Sumner, 'Double-ended Fault Location Method with Reduced Measurements Double-ended Fault Location Method with Reduced Measurements', *Proceedings of the Cardiff University Engineering Research Conference 2023*, Cardiff, UK, pp. 153-157.

doi.org/10.18573/conf1.ai

INTRODUCTION

Having a quick and accurate technique for locating faults is crucial in an integrated power system (IPS) because it reduces the time required to restore power to loads and enhances the system’s reliability [1]. Additionally, creating a fault location method that is affordable and requires minimal measurements is a challenging task to solve.

Double-ended impedance-based fault location is a widely used technique in the field of power system protection, enabling accurate and efficient fault location on distribution lines. The method is based on the measurement of impedance before and after the fault occurrence, and analysis of the difference in impedance measurements at both ends of the line to determine the location of the fault. Many studies have been conducted on the double-ended impedance-based fault location technique, demonstrating its effectiveness and reliability [2-5]. For example, a study by Aboshady (2017) [2] applied the technique to a distribution network, showing its ability to accurately locate faults even in such situations. Another study by Bahmanyar et al. (2017) [3] compared the performance of different fault location methods, demonstrating the advantage of the double-ended impedance-based method in terms of accuracy and robustness.

In summary, the double-ended impedance-based fault location technique has several advantages over other methods, including its non-intrusive nature, independence from line parameters, and ability to locate faults in both radial and meshed networks. Moreover, the technique has been implemented in studied for commercial protection relays, further demonstrating its practicality and reliability in real-world applications[4-5]. However, it requires full voltage and current measurements from both terminals of the faulted line. In this work, a double-ended impedance based with less measurements at non-fundamental frequencies is explored.

DOUBLE ENDED FAULT LOCATION METHOD (DEFLM)

In this section, a double-ended impedance based fault location method will be introduced based on full measurement and reduced measurement.

DEFLM

A single-phase circuit with a short circuit on the distribution line, is shown in Fig. 1(a), and is used to introduce the basis of this method. The supply impedance is represented by (Z_s), while Z_L is the equivalent load impedance. The cable impedance between the fault and the source end is Z_x and the remaining impedance Z_{l-x} represents the cable impedance from the fault point to the receiving end of the line. Note that the earth and the neutral are connected. The supply source at non-fundamental frequencies behaves as a short circuit, as shown in the Thevenin equivalent circuit of Fig. 1(b), while the fault is represented as a transient source which creates an equal and opposite voltage to the instantaneous pre-fault voltage (V_{pre-f}) at the fault location. POM1 is the point-of-measurement at the source end, while POM2 is the point-of-measurement at the receiving end.

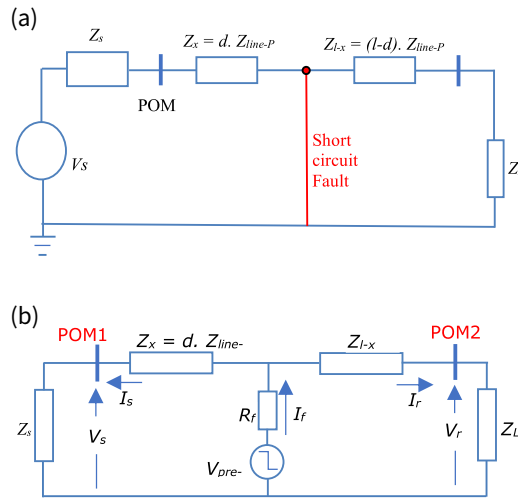


Fig. 1. Single line diagram with short circuit fault (a) Network at 50Hz, (b) Network at High frequency contents.

Kirchhoff’s laws are applied to the measured voltage and current during a fault for the measurements at both ends of the line to calculate the impedance between POM1 and the fault , yields (1) [6 - 8]:

$$V_s + I_s \cdot Z_x + I_f \cdot R_f = V_r + I_r \cdot Z_{l-x} + I_f \cdot R_f \tag{1}$$

where V_s, I_s are the voltage and current measurement at the source end of the line and V_r, I_r are the measured voltage and current at the receiving (load) end. The total impedance of the line is $Z_l = Z_x + Z_{l-x}$. Rearranging (1) for Z_x , gives (2):

$$Z_x = \frac{V_r - V_s + I_r \cdot Z_l}{I_s + I_r} \tag{2}$$

The fault distance is calculated by dividing Z_x by the per-meter impedance of the line (Z_{line-p}), as given in (3). The imaginary part of the impedance only is used because the reactance is not influenced by the fault resistance, and at higher frequencies, the reactance dominates the overall impedance more than the resistance. Furthermore, (2) shows that the fault resistance information, as well as the knowledge of the load impedance or the supply impedance are not required by the proposed DEFLM.

$$d = \frac{\text{imag}\left(\frac{V_r - V_s + I_r \cdot Z_l}{I_s + I_r}\right)}{\text{imag}(Z_{line-p})} \tag{3}$$

DEFLM, ignoring I_r

It is proposed that the DEFLM can be implemented using only three measurements. In this approach, the source end voltage and current, as well as the receiving end voltage, will be required. Equation (2) is approximated by (4), which will be used in this section.

$$Z_x = \frac{V_r - V_s}{I_s} \tag{4}$$

Compared to (2), I_r is neglected in the denominator because at non-fundamental frequencies, it is assumed that $I_r \ll I_s$. Similarly, $I_r \cdot Z_l$ in the numerator of (2) will be very small compared to , hence, neglecting it has a limited influence on the estimated reactance and hence less measurement is required.

RESULTS

A model of a simple system was created using MATLAB/Simulink software. The single line diagram of the power system fault demonstrator at the ‘Flex Elec’ Laboratory-based IPS/microgrid at the University of Nottingham is shown in Fig. 2 [7,8], while the simulated demonstrator is shown in Fig. 3. The system consists of four sections with zone 1, 2 and 4 of 10m in length while zone 3 is 20 m. Each section is represented by lumped series resistance and inductance while the line capacitance is ignored due to the size and length of the cable used in the demonstrator. The current limiter and the load are also represented by pure resistance and inductance in series whereas the busbar and the power transformer are represented by a simple AC supply as shown in Fig. 3.

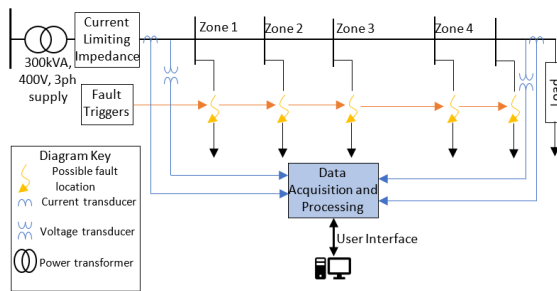


Fig. 2. Fault demonstrator at the University of Nottingham.

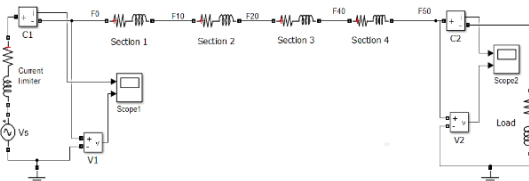


Fig. 3. MATLAB simulation of the Fault Demonstrator.

The per-unit-length resistance and inductance for each section are 1.15 mΩ/m and 0.82 μH/m [6-7], respectively. The load magnitude is (22+0.157j) Ω and the current limiting impedance is (0.5 + 0.0157j) Ω at 50Hz. Voltage and current transients measured at both ends, as shown in Fig. 4, are captured for 10ms at a sampling frequency of 50 kHz. The signals are then processed by multiplying it with a Blackman window. Finally, a Fast Fourier Transform (FFT) is used to transform the time domain signals to frequency domain and these are then used in (3). The frequency domain representation of these transients are derived using the FFT from the time domain signals and are shown in Fig. 5 with a frequency range up to 5 kHz.

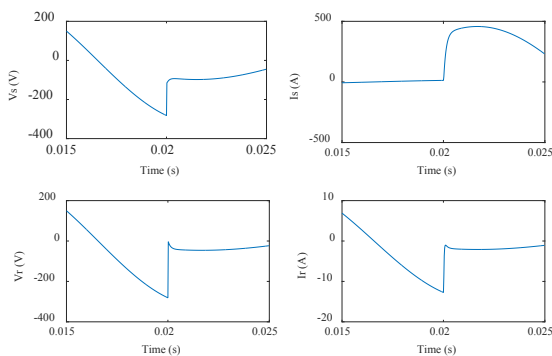


Fig. 4. Captured signals from POM1 and POM2 of the Simulated model.

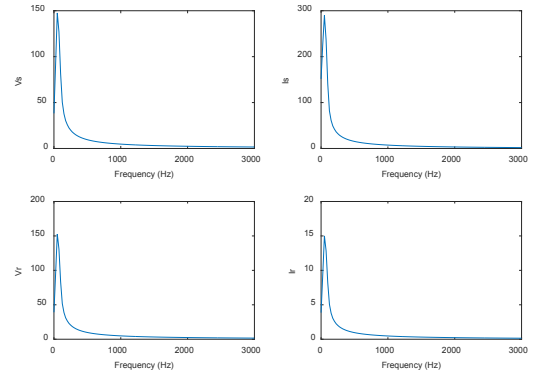


Fig. 5. Normalised Frequency domain representation of the measured signals from POM1 and POM2.

DEFLT Results

Five locations have been selected to create a line to ground fault through a 0.1Ω resistance as marked in Fig. 3: F0, F10, F20, F40, and F50. F0 represents a fault at the source end (POM1) while F50 is a fault at the receiving (POM2) end which is 50m from the source end. The data window is selected so that the fault transient is at the centre of the captured window as shown in Fig. 4. 5ms of pre-fault and 5ms of during-fault of data is utilized for the fault location algorithm.

The impedance estimated for the five fault locations in the frequency domain up to 3 kHz is shown in Fig. 6(a) which is the imaginary part while Fig. 6(b) is the real part of the impedance.

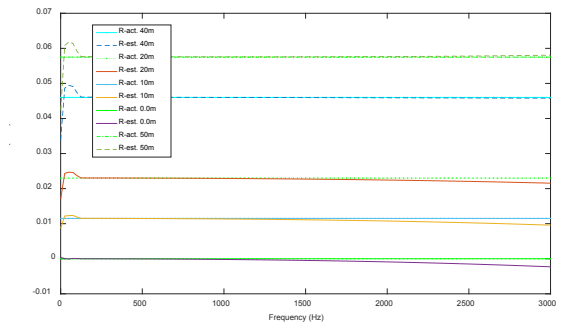
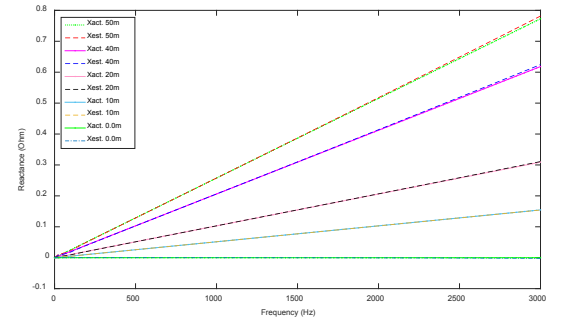


Fig. 6 Estimated impedance using DEFLM (a) Inductance part of the estimated Impedance (top), and (b) resistance part of the estimated impedance (bottom).

These estimated magnitudes represent the value of impedance between the source end and the fault location at non-fundamental frequencies, which is as indicated in Fig. 1. The solid lines represent the actual values used in

the model (Xact.), while the dashed lines are the estimated values (Xest.) using the DEFLM. It was found that the technique regarding the reactance part shows a strong match between estimated and actual values in the higher frequency range up to 3000 Hz while the resistance shows poorer accuracy than the reactance in the high frequency range. This is because in the high frequency range, the reactance is many times bigger than the resistance and any small error in the angle identified by the FFT process causes a significant error in the estimated resistance. However, the resistance can be ignored because the value of reactance is much higher than the resistance. Hence, the reactance is selected to locate the fault by dividing it with the per-metre reactance of the line at different frequencies.

DEFLM, ignoring I_r results

In this section, the DEFLT with one less measurement will be investigated. Receiving end current (I_r) is dropped and equation (4) is used to estimate the distance and consequently the distance.

Two line-neutral fault tests (F20 and F40) are imposed with $R_f = 4.5\Omega$ in order to demonstrate this approach. In Fig. 7 shown for F20, the estimated reactance using (4) (the solid blue line) is compared to the estimation using (2) (the dash-dotted red line). There is an obvious match between the two estimations. There is a small reduction in the accuracy when a fault was imposed 40m from the source-end (F40), which is shown in Fig. 8. However, the increase in the percentage error is less than 1%.

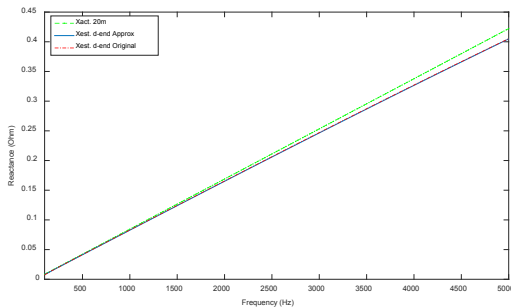


Fig.7. Estimated reactance using (2) versus (4) for fault at 10m.

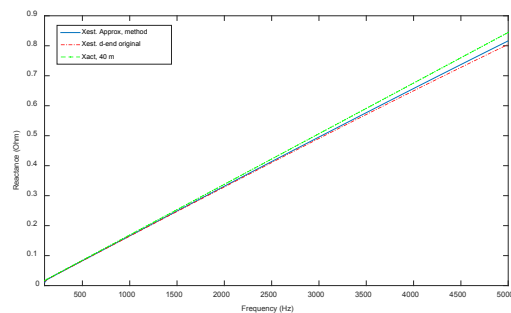


Fig. 8. Estimated reactance using (2) versus (4) for fault at 40m.

This behaviour is verified by looking at the frequency domain of the signals using in Fig. 9 which shows that $I_r(f) \ll I_s(f)$ as well as $I_r * Z_l \ll V_r - V_s$. Figure 9 shows the frequency domain representation of the measured signals for fault at 10m (top) I_s , I_r and $I_s + I_r$; and (bottom) $V_r - V_s$, $I_r * Z_l$, and $V_r - V_s + I_r * Z_l$.

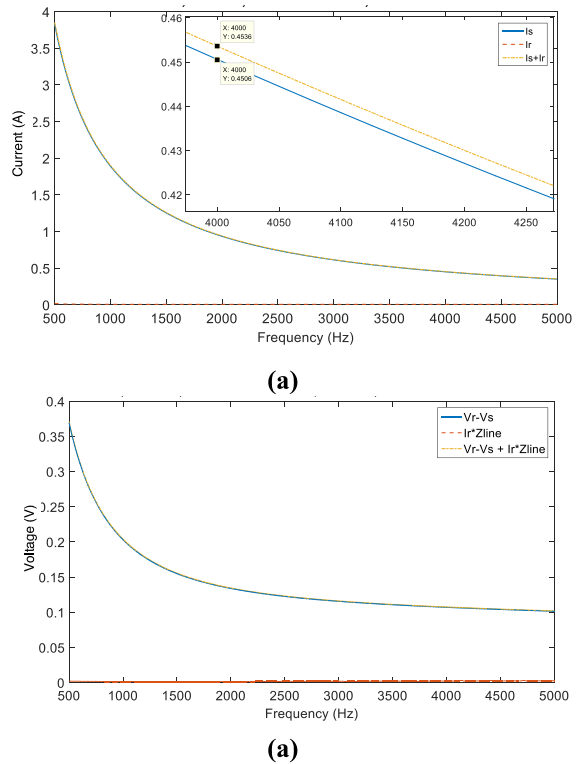


Fig.9. Frequency domain representation of the measured signals for fault at 10m.

CONCLUSIONS

A DEFLM based on higher frequency content of the fault generated transient utilizing full two ends measurements and reduced measurements is introduced and investigated. It has been shown that the DEFLM shows a very high accuracy when locating fault using the voltage and current measurements from the two terminals. Additionally, the proposed approach by reducing the required measurements from the load end, showed that the accuracy can drop. However, the accuracy of the proposed approach is still within acceptable rate.

Acknowledgments

This work was partially supported by EPSRC [Grant Number: EP/T021780/1].

Conflicts of interest

The authors declare no conflict of interest.

REFERENCES

- [1] R. Dashti, M. Daisy, H. Mirshekali, H. R. Shaker, and M. Hosseini Aliabadi, 'A survey of fault prediction and location methods in electrical energy distribution networks', *Measurement*, vol. 184, p. 109947, Nov. 2021. doi.org/10.1016/j.measurement.2021.109947
- [2] F. M. Aboshady, M. Sumner, and D. W. P. Thomas, 'A double end fault location technique for distribution systems based on fault-generated transients', in *2017 IEEE 26th International Symposium on Industrial Electronics (ISIE)*, Edinburgh, United Kingdom: IEEE, Jun. 2017, pp. 32–36. doi.org/10.1109/ISIE.2017.8001219
- [3] A. Bahmanyar, S. Jamali, A. Estebarsari, and E. Bompard, 'A comparison framework for distribution system outage and fault location methods', *Electric Power Systems Research*, vol. 145, pp. 19–34, Apr. 2017. doi.org/10.1016/j.epsr.2016.12.018
- [4] A. G. Phadke and J. S. Thorp, *Computer relaying for power systems*, 2nd ed., Chichester, West Sussex; Hoboken, NJ: Baldock, Hertfordshire: John Wiley & Sons; Research Studies Press, 2009.
- [5] M.M. SahaSaha, J. Izykowski, J. Rosolowski, 'Two-end and Multi-end Fault-location Algorithms', in *Fault Location on Power Networks*, London: Springer London, 2010, pp. 263–331. doi.org/10.1007/978-1-84882-886-5_7
- [6] H. K. Jahanger, M. Sumner, and D. W. P. Thomas, 'Combining fault location estimates for a multi-tapped distribution line', in *2017 IEEE PES Innovative Smart Grid Technologies Conference Europe (ISGT-Europe)*, Torino, Italy: IEEE, Sep. 2017, pp. 1–6. doi.org/10.1109/ISGTEurope.2017.8260187
- [7] H. K. Jahanger, D. W. P. Thomas, M. Sumner, and C. Rose, 'Impact of an inverter-based DG on a double-ended fault location method', *The Journal of Engineering*, vol. 2018, no. 15, pp. 1078–1083, Oct. 2018. doi.org/10.1049/joe.2018.0261
- [8] H. K. Jahanger, D. W. P. Thomas, and M. Sumner, 'An investigation into the robustness of a double-ended wideband impedance-based fault location technique', *Scientific Reports*, vol. 13, no. 1, p. 10001, Jun. 2023. doi.org/10.1038/s41598-023-36541-2

Proceedings of the Cardiff University Engineering Research Conference 2023 is an open access publication from Cardiff University Press, which means that all content is available without charge to the user or his/her institution. You are allowed to read, download, copy, distribute, print, search, or link to the full texts of the articles in this publication without asking prior permission from the publisher or the author.

Original copyright remains with the contributing authors and a citation should be made when all or any part of this publication is quoted, used or referred to in another work.

E. Spezi and M. Bray (eds.) 2024. *Proceedings of the Cardiff University Engineering Research Conference 2023*. Cardiff: Cardiff University Press.
doi.org/10.18573/conf1

Cardiff University Engineering Research Conference 2023 was organised by the School of Engineering and held from 12 to 14 July 2023 at Cardiff University.

The work presented in these proceedings has been peer reviewed and approved by the conference organisers and associated scientific committee to ensure high academic standards have been met.

First published 2024

Cardiff University Press
Cardiff University, PO Box 430
1st Floor, 30-36 Newport Road
Cardiff CF24 0DE

cardiffuniversitypress.org

Editorial design and layout by
Academic Visual Communication

ISBN: 978-1-9116-5349-3 (PDF)



This work is licensed under the Creative Commons Attribution - NoCommercial - NoDeriv 4.0 International licence.

This license enables reusers to copy and distribute the material in any medium or format in unadapted form only, for noncommercial purposes only, and only so long as attribution is given to the creator.

<https://creativecommons.org/licenses/by-nc-nd/4.0/>